Configuration spaces of convex and embedded polygons in the plane

Don Shimamoto* and Mary Wootters†

A celebrated result of Connelly, Demaine, and Rote [**6**] states that any polygon in the plane can be "convexified." That is, the polygon can be deformed in a continuous manner until it becomes convex, all the while preserving the lengths of the sides and without allowing the sides to intersect one another. In the language of topology, their argument shows that the configuration space of *embedded* polygons with prescribed side lengths deformation retracts onto the configuration space of *convex* polygons having those side lengths. In particular, both configuration spaces have the same homotopy type. Connelly, Demaine, and Rote observe (without proof) that the space of convex configurations is contractible. Separately, work of Lenhart and Whitesides [**10**] and of Aichholzer, Demaine, Erickson, Hurtado, Overmars, Soss, and Toussaint [**1**] had shown that the space of convex configurations is connected. These results are part of the literature on linkages. The polygons here are mechanical linkages in which the sides can be viewed as rigid bars of fixed length arranged in a cycle and the vertices as joints about which the bars can rotate.

In this note we determine the topology of the space of convex configurations and the space of embedded configurations up to homeomorphism. We regard two polygons as equivalent if one can be translated and rotated onto the other. After a translation, we may assume that one of the vertices is at the origin and then, after a rotation, that one of the adjacent sides lies along the positive x-axis. To fix some notation, let $\vec{\ell} = (\ell_1, \ldots, \ell_n)$ be a given sequence of side lengths, where $\ell_i > 0$ for all i and $n \geq 3$. The configuration space of planar polygons with these side lengths is defined by:

$$X(\vec{\ell}) = \{(p_1, \ldots, p_n) \in (\mathbf{R}^2)^n \ : \ p_1 = (\ell_1, 0), p_n = (0,0), \text{ and } |p_i - p_{i-1}| = \ell_i \text{ for } i = 1, \ldots, n\}.$$

Here, and in what follows, subscripts should be taken modulo n where appropriate. Also, to simplify the notation, we suppress the dependence on $\vec{\ell}$, writing X rather than $X(\vec{\ell})$. Note that X inherits a natural topology as a subspace

*Department of Mathematics and Statistics, Swarthmore College, 500 College Ave., Swarthmore, PA 19081. dshimam1@swarthmore.edu.

†Department of Mathematics and Statistics, Swarthmore College, 500 College Ave., Swarthmore, PA 19081. mary.wootters@gmail.com. Supported by a Swarthmore College Summer Research Fellowship.

of $(\mathbf{R}^2)^n$. To any element $p = (p_1, \ldots, p_n)$ in X we associate its sequence of *turn angles* $\theta = (\theta_1, \ldots, \theta_n)$, where θ_i is the signed angle at p_i from the ith edge $e_i = p_i - p_{i-1}$ to the $(i+1)$th edge $e_{i+1} = p_{i+1} - p_i$. We choose θ_i to lie in the interval $(-\pi, \pi]$. A positive value of θ_i corresponds to a left turn, and a negative value to a right turn.

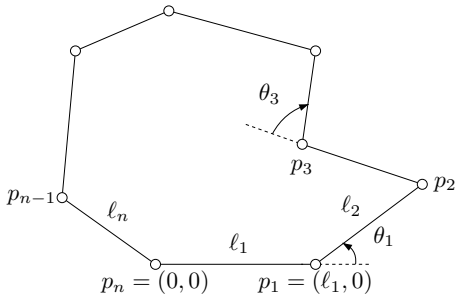

Figure 1: A polygon in the plane with vertices, side lengths, and turn angles labeled.

The definition of X permits polygons that intersect themselves. We exclude such configurations by focusing on embedded polygons, that is, those in which the edges do not intersect except at common endpoints. These polygons fall into two components depending on whether they are traversed counterclockwise ($\sum_i \theta_i = 2\pi$) or clockwise ($\sum \theta_i = -2\pi$). The two components are homeomorphic to one another by the transformation that sends each polygon to its reflection in the x-axis. Here we concentrate on the counterclockwise component:

0.1. *Let X_E denote the set of polygons $p = (p_1, \ldots, p_n)$ in X that are embedded in $\mathbf{R}^2$ and satisfy $\sum_i \theta_i = 2\pi$.*

Within X_E is the subset of convex configurations:

0.2. *Let X_C denote the subset of X_E consisting of convex polygons.*

These are the elements of X_E whose turn angles satisfy $\theta_i \geq 0$ for all i.

The topology of the configuration space X has been studied using a variety of techniques by several authors (for instance, Hausmann [**7**], Kamiyama [**8**], and Kapovich and Millson [**9**]). The analysis can get complicated, but certain basic properties are easy to establish. For instance, suppose that X contains no straight line configurations, that is, no configurations in which all the edges lie along a single line. This is the generic situation, since X contains a straight line configuration if and only if it is possible to choose values $\epsilon_i = \pm 1$ such that $\sum_i \epsilon_i \ell_i = 0$. Then it is well known that X is a C^∞ compact orientable manifold of dimension $n - 3$ (see Shimamoto and Vanderwaart [**12**] for a recent exposition). The space of embedded polygons X_E is an open subset of X, hence

also an $(n-3)$-dimensional manifold. The space of convex configurations X_C is a closed subset of X (though not a smooth one, as we shall see). Here it is still important to exclude straight line configurations, since otherwise a sequence of convex configurations could converge to a straight line configuration, which would be a limit point not in X_C.

For the remainder of the paper, assume that the side lengths are such that X contains no straight line configurations. Our main results describe the topological type of X_C and X_E. Specifically, we prove that:

0.3. *X_C is homeomorphic to a closed $(n-3)$-dimensional ball B, e.g., to $B = \{x \in \mathbf{R}^{n-3} : |x| \leq 1\}$,*

and

0.4. *X_E is homeomorphic to $\mathbf{R}^{n-3}$.*

Statement (0.3) is proved in section 1 (where it is called Theorem 5), and (0.4) is proved in section 2 (Theorem 7). We close in section 3 with a counterexample to a conjecture of Connelly, Demaine, and Rote regarding the closure of X_E in X.

1 Convex configurations

A polygon $p = (p_1, \ldots, p_n)$ in X has a sequence of turn angles $\theta = (\theta_1, \ldots, \theta_n)$ in $\mathbf{R}^n$. But conversely the turn angles determine the polygon as well, since $p_1 = (\ell_1, 0)$ by our convention and, for $j > 1$,

$$p_j = p_{j-1} + \ell_j\big(\cos(\sum_{k=1}^{j-1}\theta_k)\,,\,\sin(\sum_{k=1}^{j-1}\theta_k)\big).$$

In this section we will be concerned only with convex polygons, in which case $\theta_i \in [0, \pi)$ for all i. This eliminates any worries about continuity problems modulo 2π as the angles vary. Thus the function $t(p_1, \ldots, p_n) = (\theta_1, \ldots, \theta_n)$ that sends a polygon to its turn angles maps the subspace X_C of convex configurations homeomorphically onto its image $\mathcal{S} = t(X_C)$ in $\mathbf{R}^n$. The set $\mathcal{S}$ consists of all sequences of turn angles that are realized by convex polygons with side lengths $\vec{\ell}$. We will determine the topological type of X_C by studying how it is parametrized by $\mathcal{S}$, essentially executing a search of all possible turn angles. Actually, a convex polygon is determined by its first $n-3$ turn angles alone, but for our arguments it is convenient to keep track of all n of them.

The general strategy here is to examine inductively how much freedom there is to rotate each of the edges. For instance, the first edge is fixed from $p_0 = p_n = (0, 0)$ to $p_1 = (\ell_1, 0)$ by our convention. We then see how much the second edge can be "wiggled" under the restriction that the whole polygon remains convex. For each position reached by this motion, we see how much the next edge can be wiggled, and so forth. By doing this for all the edges (or at least

for the first $n-2$ of them), all configurations will have been visited. We show that each of the wiggle ranges is an interval, which is nontrivial except possibly when one of the previous positions was set to an interval endpoint. Moreover, the endpoints of these intervals vary continuously with the angle choices in the positions that precede it. Thus the space of convex configurations can be built up iteratively as a union of segments of continuously varying length.

1.1 The maximum and minimum turn angles

For $k \le n$, let $\pi_k \colon \mathbf{R}^n \to \mathbf{R}^k$ be the projection onto the first k coordinates, $\pi_k(x_1, \ldots, x_n) = (x_1, \ldots, x_k)$, and let $\mathcal{S}_k = \pi_k(\mathcal{S})$. In words,

$$\begin{aligned}\mathcal{S}_k = \{&(\theta_1, \ldots, \theta_k) \ : \text{ there exist } \theta_{k+1}, \ldots, \theta_n \text{ such that } (\theta_1, \ldots, \theta_n) \text{ is the} \\ &\text{sequence of turn angles of a convex polygon } p\}.\end{aligned}$$

We determine the topology of $\mathcal{S}$ by analyzing the relation between $\mathcal{S}_k$ and $\mathcal{S}_{k-1}$ inductively.

For example, $\mathcal{S} \approx X_C$ is connected [**1**], [**10**] and compact, so, since π_1 is continuous, $\mathcal{S}_1$ is a finite closed interval, say

$$\mathcal{S}_1 = [\nu_1, \mu_1]. \tag{1.1}$$

Here μ_1 represents the maximum possible turn angle at p_1, and ν_1 represents the minimum.

In general, if $k > 1$, let $\alpha = (\alpha_1, \ldots, \alpha_{k-1})$ in $\mathcal{S}_{k-1}$ be given. These turn angles determine a fixed chain of k edges from p_0 to p_k. Define

$$R_k(\alpha) = \{\theta_k \in \mathbf{R} \ : \ (\alpha, \theta_k) \in \mathcal{S}_k\}.$$

This represents the wiggle room mentioned earlier for the $(k+1)$th edge, given fixed positions for the first k edges. Next let

$$\nu_k(\alpha) = \inf R_k(\alpha) \qquad \text{and} \qquad \mu_k(\alpha) = \sup R_k(\alpha).$$

These are the smallest and largest possible turn angles at p_k, again assuming an initial fixed chain up to that point is given.

We will describe various properties of ν_k and μ_k including the fact that they are actually attained, that is, $\nu_k(\alpha), \mu_k(\alpha) \in R_k(\alpha)$, by deforming our polygons into certain standard configurations. In some cases, we sketch details of proofs when the geometry is clear, making particular use of the observations in Aichholzer et al. [**1**], for instance:

Lemma 1. *Given a convex quadrilateral with vertices v_1, v_2, v_3, v_4, there is a motion that increases the turn angles at v_1 and v_3 and decreases the turn angles at v_2 and v_4 while preserving the lengths of the sides. The motion can continue until one of the turn angles reaches 0 or π.*

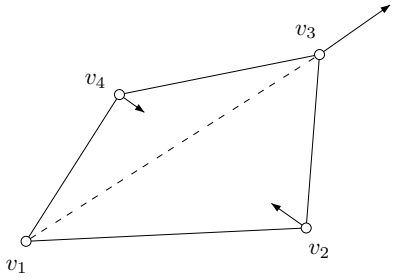

Figure 2: Increasing the turn angles at v_1 and v_3 and decreasing the turn angles at v_2 and v_4.

The idea is to move v_3 directly away from v_1 along the ray from v_1 to v_3. (See Figure 2.) The positions of v_2 and v_4 are then determined by the side lengths. The authors in [**1**] use this result to show that, given any two convex polygons with the same sequence of edge lengths, there is a continuous motion from one to the other in which all angles change monotonically. The monotonicity ensures that the intermediate polygons are also convex, whence the space X_C is connected.

For convenience, we introduce the following terminology.

Definition. In a polygon $(p_1, \ldots, p_n)$ with turn angles $(\theta_1, \ldots, \theta_n)$, a vertex p_i is called *flat* if $\theta_i = 0$.

Now consider the minimum turn angle $\nu_k(\alpha)$. If there exists a polygon having turn angles $(\alpha, \theta_k, \ldots, \theta_n)$ with $\theta_k = 0$, then $\nu_k(\alpha) = 0$, since that's always the smallest possible turn angle for a convex polygon. Let us call this case (a). Otherwise, suppose that $\theta_k > 0$. To decrease this turn angle, we try to rotate the $(k+1)$th edge clockwise. If the subchain from p_{k+1} to p_n is not straight, choose a vertex p_j along the way such that the turn angle θ_j is nonzero, Now consider the quadrilateral $p_n p_k p_{k+1} p_j$. By keeping the subchains of the original polygon between these vertices rigid and moving p_{k+1} directly away from p_n as described above, we reduce the turn angle θ_k. (See Figure 3(i). In the figure, as the inscribed quadrilateral flattens, the subchains between its vertices will rotate. Strictly speaking, this violates our convention that edge $p_n p_1$ lie along the positive x-axis, so one should imagine a simultaneous compensating global rotation that keeps $p_n p_1$ horizontal.) Continue until either $\theta_k = 0$ or one of the vertices along the subchain becomes flat. In the case of the latter, if the subchain from p_{k+1} to p_n is still not straight, repeat. In this way, we eventually reach a configuration in which either $\theta_k = 0$ (case (a) again, as in Figure 3(ii)) or the subchain from p_{k+1} to p_n is straight (call this case (b), shown in Figure 3(iii)). We refer to a configuration of either of these types as *minimally stretched*. (For case (a), there is not a unique such configuration, but this does not matter for our arguments.) The procedure just given shows that, in a minimally stretched configuration, $\theta_k = \nu_k(\alpha)$, since the turn angle θ_k of any other polygon can be

reduced until it reaches such a configuration. This also implies that $R_k(\alpha)$ is connected.

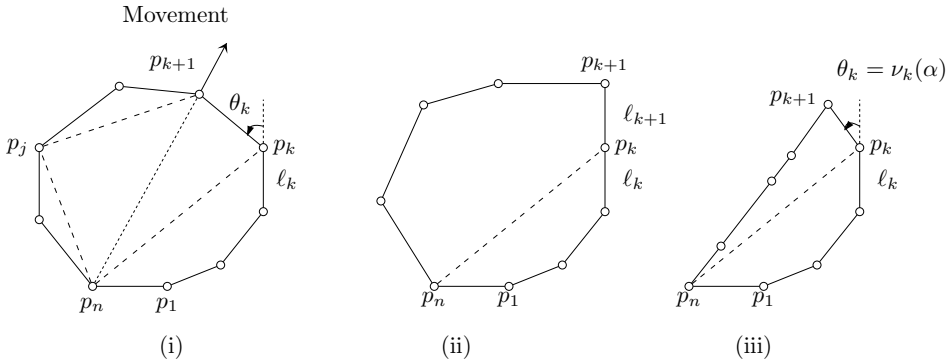

Figure 3: (i) Reducing θ_k; (ii) case (a): $\nu_k(\alpha) = 0$; (iii) case (b): $\nu_k(\alpha) > 0$

Finally we claim that $\nu_k(\alpha)$ is a continuous function of α, that is, a small change in the initial subchain produces a small change in the minimum turn angle. This is clear except possibly at the overlap of cases (a) and (b), that, is, when $\nu_k(\alpha) = 0$ and the subchain from p_{k+1} to p_n is straight (Figure 4). Here a small change in α can lead either to case (a) or (b), but either way the minimally stretched configuration changes only slightly, and hence so does the minimum turn angle.

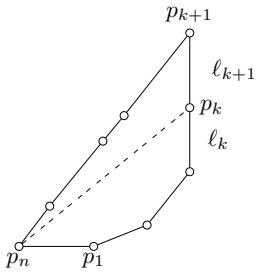

Figure 4: Borderline case.

The case of the maximum turn angle $\mu(\alpha)$ is similar, only now we want to rotate the $(k+1)$th edge counterclockwise as far as possible. We do this by trying to straighten the back end of the polygon as much as we can, pulling the edge towards it in the process. To make this more precise, let a configuration with turn angles $(\alpha, \theta_k, \ldots, \theta_n)$ be given. If the subchain from p_k to p_{n-1} is not straight, choose a vertex p_j along the way for which $\theta_j \neq 0$. Now consider the quadrilateral $p_n p_k p_j p_{n-1}$. By moving p_{n-1} directly away from p_k, we increase the turn angle θ_k (Figure 5(i)). Continue until, in the original polygon, either

one of the vertices along the subchain becomes flat or p_n becomes flat. In the first case, if the subchain from p_k to p_{n-1} is still not straight, repeat the procedure. On the other hand, if p_n is flat, repeat with p_{n-1} in place of p_n and look at the subchain from p_k to p_{n-2}. Eventually, one reaches a configuration in which the subchain from p_k to p_j is straight for some $j > k$ and the vertices from p_{j+2} to p_n, if any, are flat. Let us call such a configuration *maximally stretched* (Figure 5(ii)). In particular, at most two vertices from p_{k+1} to p_n are not flat, and, if there are two, they are adjacent to one another.

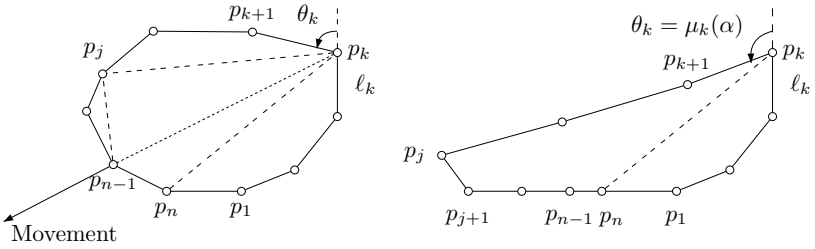

(i) (ii)

Figure 5: (i) Increasing θ_k; (ii) maximally stretched configuration.

As with ν_k, in a maximally stretched configuration $\theta_k = \mu_k(\alpha)$ because any polygon can be deformed to such a configuration with θ_k increasing along the way. In addition, $\mu_k(\alpha)$ varies continuously with α. This time, the borderline case is when the subchains from p_k to p_j and from p_j to p_1 are both straight. When this happens, a small change in α can lead to maximally stretched configurations with straight subchains either from p_k to p_j or from p_k to p_{j-1}. While this description may sound discontinuous, the maximally stretched configurations themselves change only slightly, and hence so does $\mu_k(\alpha)$.

To recap, we have shown that $R_k(\alpha) = [\nu_k(\alpha), \mu_k(\alpha)]$. Since by definition, $\mathcal{S}_k = \{(\alpha, \theta_k) \in \mathbf{R}^k \mid \alpha \in \mathcal{S}_{k-1}, \theta_k \in R_k(\alpha)\}$, the preceding discussion can be summarized as follows.

Lemma 2. *There exist real numbers ν_1 and μ_1 such that $\mathcal{S}_1 = [\nu_1, \mu_1]$, and, for $k > 1$, there exist continuous functions $\nu_k, \mu_k \colon \mathcal{S}_{k-1} \to \mathbf{R}$ such that*

$$\mathcal{S}_k = \{(\alpha, \theta_k) \in \mathbf{R}^k \ : \ \alpha \in \mathcal{S}_{k-1}, \nu_k(\alpha) \le \theta_k \le \mu_k(\alpha)\}. \tag{1.2}$$

In other words, $\mathcal{S}_k$ is the region over $\mathcal{S}_{k-1}$ lying between two continuous graphs.

1.2 The topology of $\mathcal{S}_k$.

To complete the description of the topology of $\mathcal{S}_k$, we use one final technical lemma.

Lemma 3. *Suppose that $2 \le k \le n-3$. If $\alpha \in \operatorname{Int} \mathcal{S}_{k-1}$, then $\nu_k(\alpha) < \mu_k(\alpha)$.*

Here the interior of $\mathcal{S}_{k-1}$ is as a subset of $\mathbf{R}^{k-1}$.

Proof. Suppose to the contrary that $\nu_k(\alpha) = \mu_k(\alpha)$. In other words, given the initial subchain from p_0 to p_k, the polygon is completely rigid. Thus there exists a polygon with turn angles $(\alpha, \theta_k, \ldots, \theta_n)$ that is simultaneously minimally and maximally stretched. We consider two cases.

First, suppose that $\theta_k = 0$ (Figure 6(i)). Then the straight subchain from p_k to p_j that is part of a maximally stretched configuration is contained in a straight subchain from p_{k-1} to p_j. Hence, this configuration is maximally stretched at p_{k-1} as well, that is, $\alpha_{k-1} = \mu_{k-1}(\alpha_1, \ldots, \alpha_{k-2})$. By (1.2), this contradicts the assumption that $\alpha \in \operatorname{Int} \mathcal{S}_{k-1}$.

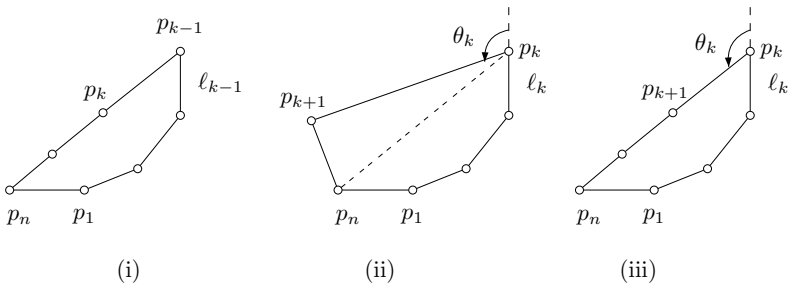

Figure 6: $\theta_k = \nu_k(\alpha) = \mu_k(\alpha)$: (i) $\theta_k = 0$; (ii) $\theta_k > 0$, p_{k+1} not flat; (iii) $\theta_k > 0$, p_{k+1} flat.

On the other hand, suppose that $\theta_k > 0$. Then, as a minimally streched configuration, the subchain from p_{k+1} to p_n is straight. If p_{k+1} is not flat (Figure 6(ii)), then, as part of a maximally stretched configuration, this subchain can consist of at most one edge. Thus $k \geq n - 2$, contrary to assumption. But if p_{k+1} is flat, then the entire subchain from p_k to p_n is straight, meaning that the configuration is minimally stretched at p_{k-1}, i.e. $\alpha_{k-1} = \nu(\alpha_1, \ldots, \alpha_{k-2})$, again contradicting $\alpha \in \operatorname{Int} \mathcal{S}_{k-1}$ (Figure 6(iii)).

In all cases we reach a contradiction. □

From this we obtain the topological type of $\mathcal{S}_k$.

Proposition 4. *If $1 \leq k \leq n - 3$, then $\mathcal{S}_k$ is homeomorphic to a closed k-dimensional Euclidean ball.*

Proof. We use induction on k. For $k = 1$, the result is given by (1.1). If $k > 1$, we use (1.2). By induction, we may replace $\mathcal{S}_{k-1}$ by a closed $(k-1)$-dimensional ball, up to homeomorphism (Figure 7(i)). Let $\partial\mathcal{S}_{k-1}$ denote the boundary of $\mathcal{S}_{k-1}$, a topological $(k-2)$-dimensional sphere. Let A denote the graph of ν_k restricted to $\partial\mathcal{S}_{k-1}$, i.e., $A = \{(\alpha, \nu_k(\alpha)) : \alpha \in \partial\mathcal{S}_{k-1}\}$. Similarly, let B denote the graph of μ_k restricted to $\partial\mathcal{S}_{k-1}$. Choose some large number $M > 0$, and construct two cones, C_1 from A to the point $(0, \ldots, 0, -M) \in \mathbf{R}^k$ and C_2 from B to the point $(0, \ldots, 0, M)$ (Figure 7(ii)).

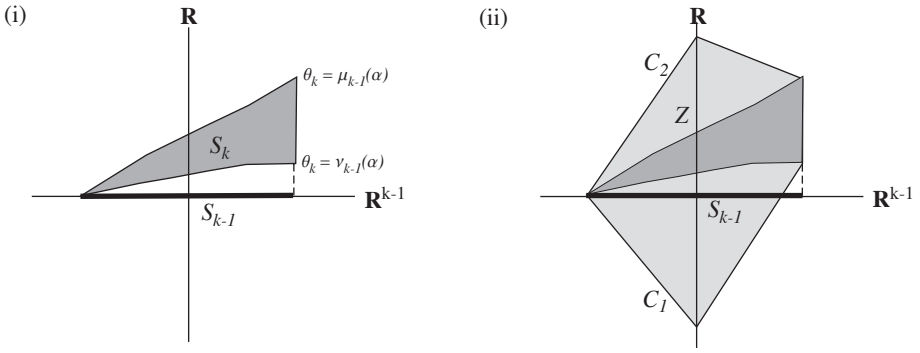

Figure 7: (i) $\mathcal{S}_k$ over $\mathcal{S}_{k-1}$, (ii) region between two cones.

Let Z be the region over $\mathcal{S}_{k-1}$ lying between these two cones. Then $\mathcal{S}_k$ can be mapped homeomorphically onto Z by taking each "vertical" interval $\alpha \times R_k(\alpha)$ in $\mathcal{S}_k$ and dilating it in the θ_k-direction until it lies between the two cones. Note that this dilation always makes sense when $\alpha \in \operatorname{Int} \mathcal{S}_{k-1}$ by Lemma 3, and no dilation is necessary when $\alpha \in \partial\mathcal{S}_{k-1}$. Finally, Z is star-shaped in $\mathbf{R}^k$ with respect to the origin, so by radial projection it maps homeomorphically onto a closed k-dimensional ball, completing the proof. □

As mentioned earlier, a convex polygon is determined by its first $n-3$ turn angles, so $X_C \approx \mathcal{S}$ is homeomorphic to $\mathcal{S}_{n-3}$. As a corollary to Proposition 4 we obtain the main result of this section:

Theorem 5. *Assume that the configuration space $X(\vec{\ell})$ contains no straight line configurations. Then the space X_C of convex polygons with side lengths $\vec{\ell}$ is homeomorphic to a closed Euclidean ball of dimension $n-3$.*

2 Embedded configurations

We now determine the topology of the space X_E of embedded configurations. To do so, we use the following characterization of Euclidean space (see Brown [**2**] and Milnor [**11**]):

2.1. *Let M be an n-dimensional manifold such that every compact subset is contained in an open set homeomorphic to $\mathbf{R}^n$. Then M itself is homeomorphic to $\mathbf{R}^n$.*

To apply this to X_E, we proceed in two steps. First we show that the subspace X_C of convex configurations has an open neighborhood U homeomorphic to $\mathbf{R}^{n-3}$. Then given any compact subset K of X_E, we adapt the techniques of Cantarella, Demaine, Iben, and O'Brien [**4**] to stretch U so that it covers K by expanding it along the lines of gradient flow of a suitable "energy" function.

2.1 Putting a collar on the space of convex configurations

According to Theorem 5, the space X_C of convex configurations is homeomorphic to a closed $(n-3)$-ball, which makes it reasonable to expect that X_C can be thickened slightly within X_E to obtain a neighborhood homeomorphic to an open ball, hence to $\mathbf{R}^{n-3}$. We verify this by attaching a collar around X_C. The existence of such a collar would follow from standard results in differential topology if X_C were a smooth submanifold of X_E. While the result here might also follow from general considerations, we give a direct argument instead that the singularities are mild enough that a collar may still be obtained.

A subspace A of a topological space X is said to be *bicollared* if there exists an embedding $h\colon A \times (-1,1) \to X$ such that $h(a,0) = a$ for all a in A. Let ∂X_C denote the boundary of X_C in X_E. It consists of convex configurations in which at least one turn angle is zero, and it separates the nonconvex configurations in X_E from those convex configurations whose turn angles are all strictly positive. By work of Brown [**3**, p. 337] and Connelly [**5**, p. 180], in order to prove that ∂X_C is bicollared in X_E, it suffices to prove that it is bicollared locally. Thus we need only find a suitable local model of how ∂X_C sits inside X_E. We do this by identifying local coordinates. Recall that the dimension of X_E is $n-3$, so that's the number of coordinates we're looking for.

Let $a = (a_1, \ldots, a_n)$ be a given polygon in ∂X_C with turn angles $\alpha = (\alpha_1, \ldots, \alpha_n)$. These are to be regarded as fixed for the remainder of this section. Any neighborhood of a in X_E contains nonconvex configurations, since some α_i is zero and there will be nearby configurations for which the corresponding turn angle θ_i is negative. On the other hand, if $\alpha_j > 0$, we may assume that all nearby configurations also satisfy $\theta_j > 0$. The local picture depends on which of the α_i are zero. We show that $n-3$ of the turn angles, including those for which $\alpha_i = 0$, can be used to specify configurations in a neighborhood of a uniquely.

Since a is not a straight line configuration, at least three of its turn angles are nonzero, say $\alpha_q, \alpha_r, \alpha_s \neq 0$ where $1 \leq q < r < s \leq n$. In addition, a is convex, so vertex a_r does not lie on the line through a_q and a_s. Hence, the ordered triple of vertices a_q, a_r, a_s has a well-defined orientation (e.g., clockwise or counterclockwise), and we may assume that, in all sufficiently close configurations $p = (p_1, \ldots, p_n)$, the triple p_q, p_r, p_s has this same orientation as well.

We show that the $n-3$ turn angles θ_i, $i \neq q, r, s$, work as local coordinates for X_E near a, that is, a given set of values $\theta_i \approx \alpha_i$ for these angles uniquely determines a configuration $p = (p_1, \ldots, p_n)$ near a. Certainly the given angles determine the three subchains from p_q to p_r, from p_r to p_s, and from p_s to p_q, up to rotation and translation (Figure 8). We must show that these subchains can be attached to one another in only one way to form a polygon. In fact, the subchain from p_s to p_q is completely determined since it contains the fixed segment $p_n p_1$. Also, the distances $|p_q - p_r|$, $|p_r - p_s|$, and $|p_s - p_q|$ are determined by the given angles, which gives two possible locations for p_r, but only one of these has the proper orientation of p_q, p_r, p_s. Hence, the entire configuration p is uniquely determined, and we may parametrize a neighborhood of a in X_E by an open set W in $\mathbf{R}^{n-3}$.

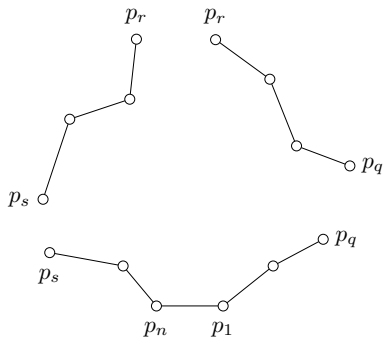

Figure 8: Three subchains determined by turn angles $\theta_i, i \neq q, r, s$.

As mentioned earlier, the local description of X_C near a depends on how many of the turn angles α_i are zero. Up to homeomorphism, we may permute the coordinates in W so that the coordinates for which $\alpha_i = 0$ come first. Say there are k such coordinates. Then by a further change of variables, we may assume that a corresponds to the point $(0, \ldots, 0, \frac{1}{2}, \ldots, \frac{1}{2})$ with an initial string of k zeros and that W itself is the open set

$$W = (-1,1) \times \cdots \times (-1,1) \times (0,1) \times \cdots (0,1) = (-1,1)^k \times (0,1)^{n-3-k}.$$

As far as the topology is concerned, the choice of intervals is arbitrary, but we are trying to draw a distinction between those coordinates for which the turn angle can be zero and those for which it cannot. Recall that the "missing" turn angles $\theta_q, \theta_r, \theta_s$ are also nonzero throughout a small enough neighborhood since we specifically selected $\alpha_q, \alpha_r, \alpha_s \neq 0$. Therefore, in these coordinates, the inclusion $X_C \subset X_E$ corresponds to

$$[0,1)^k \times (0,1)^{n-3-k} \subset (-1,1)^k \times (0,1)^{n-3-k}.$$

It is clear that the boundary of $[0,1)^k$ is bicollared in $(-1,1)^k$, hence the same remains true after taking the product with $(0,1)^{n-3-k}$. This describes the local picture and shows that ∂X_C is locally bicollared in X_E. By the results of Brown and Connelly mentioned earlier, X_C is bicollared in X_E. Since X_C is a closed $(n-3)$-ball, the union of X_C with a collar is an open $(n-3)$-ball (Figure 9). Thus we obtain the following result:

Lemma 6. *X_C has an open neighborhood U in X_E that is homeomorphic to $\mathbf{R}^{n-3}$.*

For future reference, note that by shrinking U, if necessary, we may assume that the closure $\overline{U}$ in X_E is compact.

2.2 Reconfiguration along flow lines of vector fields

In [**4**], Canterella, Demaine, Iben, and O'Brien describe a method of convexifying a polygon by decreasing its "energy." For their purposes, energy is represented by a function $F\colon X_E \to \mathbf{R}$ having the properties that:

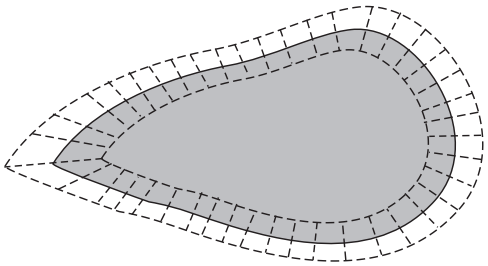

Figure 9: Ball and collar.

i. F is differentiable of class C^2 or higher;

ii. F approaches ∞ as a polygon approaches self-intersection; and

iii. F is decreasing to first order (i.e., strictly negative derivative) along strictly expansive motions. (Recall that a motion in X_E is called *strictly expansive* if the distances between all pairs of vertices do not decrease and those distances between vertices not connected by a straight chain of edges actually strictly increase, again to first order.)

Connelly, Demaine, and Rote proved that given any nonconvex configuration p in X_E a strictly expansive motion through p exists [**6**, pp. 214–227]. (On the other hand, at convex configurations, strictly expansive motions are forbidden by the Cauchy arm lemma.) Hence, according to (iii) all critical points of F lie in X_C. This, together with (ii), means that following the direction of negative gradient flow in X_E moves a polygon towards convexity.

Canterella et al. exhibit a specific energy function satisfying (i)–(iii), which they call elliptic distance energy, given by the formula:

$$F(p) = \sum_{\substack{\text{edge } \{p_i,p_{i+1}\} \\ \text{vertex } p_j \neq p_i,p_{i+1}}} \frac{1}{(|p_j - p_i| + |p_j - p_{i+1}| - |p_{i+1} - p_i|)^2}. \tag{2.2}$$

The point is that the denominator of a typical summand vanishes if and only if p_j lies on edge p_ip_{i+1}. Thus F is defined for all embedded polygons p. Moreover, in order for a polygon to self-intersect, one of the vertices must approach one of the edges and hence F goes to ∞. For our purposes, however, it simplifies the argument to modify the energy slightly.

Let $a\colon \mathbf{R} \to \mathbf{R}$ be a C^∞ function such that

$$\begin{aligned} a(x) &= 0 \quad \text{if } x \leq 0, \\ a(x) > 0 \text{ and } \frac{da}{dx}(x) &> 0 \quad \text{if } x > 0. \end{aligned}$$

A standard choice is to set $a(x) = e^{-1/x^2}$ when $x > 0$. Now given an element $p = (p_1, \ldots, p_n)$ in X_E with turn angles $\theta = (\theta_1, \ldots, \theta_n)$, define:

$$E(p) = \left(\sum_{\theta_i} a(-\theta_i) \right) \cdot F(p) \tag{2.3}$$

where F is the elliptic energy (2.2). Note that only those turn angles for which $\theta_i < 0$ contribute to the sum. Clearly E still satisfies property (i). To check (ii), suppose that p approaches self-intersection. Then at least one turn angle must approach a negative value. (Otherwise, the configurations would remain convex, approaching a straight line configuration, which is not allowed.) Therefore, the first factor in (2.3) is positive and bounded away from 0. The second factor F is known to approach ∞, and hence so does E. Lastly suppose that $\alpha(t)$ is a strictly expansive motion. This is necessarily through nonconvex configurations, so there is always at least one negative turn angle. We denote derivatives with respect to time by $\dot{(\ )}$, write $\dot{E}$ to mean $\frac{d}{dt}(E \circ \alpha)$, and likewise for other such compositions. Then

$$\dot{E} = \left(\sum_{\theta_i} -\frac{da}{d\theta}(-\theta_i) \cdot \dot{\theta}_i \right) \cdot F + \left(\sum_{\theta_i} a(-\theta_i) \right) \cdot \dot{F}. \tag{2.4}$$

In any strictly expansive motion, $\dot{\theta}_i < 0$ if $\theta_i > 0$ and $\dot{\theta}_i > 0$ if $\theta_i < 0$. This follows from, say the law of cosines and the fact that in triangle $p_{i-1}p_ip_{i+1}$ the side $|p_{i+1} - p_{i-1}|$ is strictly increasing while the sides $\ell_i = |p_i - p_{i-1}|$ and $\ell_{i+1} = |p_{i+1} - p_i|$ are fixed. Thus the first term in (2.4) is negative. By the strictly expansive property applied to F, so is the second term. Hence, $\dot{E} < 0$, showing that E satisfies (iii). This provides us with an energy function that is nonnegative on X_E and zero precisely on the subset of convex configurations X_C. In particular, by property (iii) X_C is the set of critical points.

We use this to show that X_E satisfies (2.1). Let K be a compact subset of X_E. By replacing K with $K \cup \overline{U}$, where U is the open set of Lemma 6, we may assume that $\overline{U} \subset K$. (Recall that $\overline{U}$ can be taken to be compact.) The basic idea is to let U grow outwards under the effect of the gradient of E. Perhaps it is somewhat simpler first to reverse things and to think of K flowing towards X_C under the negative gradient. This backwards flow reduces the energy of the points of K and brings them towards convexity, so after some finite amount of time τ, K is shrunk inside U. We would then like to say that, going forward in time, it follows that under positive gradient flow U is stretched so that it covers K after time τ. The stretched set would satisfy (2.1). It is certainly true that some portion of U covers K after time τ. But it is possible that some points of U fly off to infinity before time τ, so that the gradient flow is not defined on all of U over the entire interval $[0, \tau]$. As a result, we make some technical adjustments to the vector field along which the flow takes place.

Let $m = \max_{p \in K} E(p)$, and let $L = \{p \in X_E \mid E(p) \geq m + 1\}$. Then L is a closed subset of X_E such that $K \cap L = \emptyset$ (Figure 10). Using a partition of unity (which in this case reduces to the C^∞ Urysohn lemma), there exists a

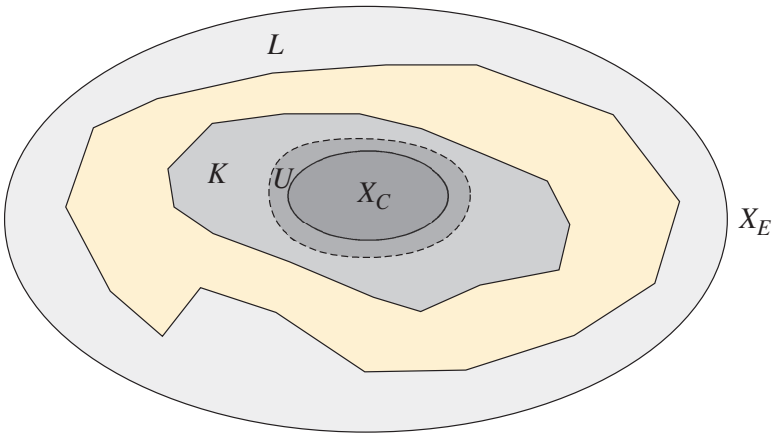

Figure 10: $X_C \subset U \subset K, K \cap L = \emptyset$. U is stretched until it covers K.

C^∞ function $b\colon X_E \to [0,1]$ such that $b = 1$ on K and $b = 0$ on L. Consider the vector field $\xi = b \cdot \operatorname{grad} E$. It agrees with $\operatorname{grad} E$ on K and vanishes on L. Let φ_t denote the flow associated to ξ. By the arguments given in the preceding paragraph, there exists a finite time $\tau > 0$ such that $\varphi_\tau(U)$ covers K. Thus $\varphi_\tau(U)$ is an open neighborhood of K homeomorphic to U, which is homeomorphic in turn to $\mathbf{R}^{n-3}$. By (2.1) this proves the following result:

Theorem 7. *Assume that the configuration space $X(\vec{\ell})$ contains no straight line configurations. Then the space X_E of embedded polygons with side lengths $\vec{\ell}$ is homeomorphic to the Euclidean space $\mathbf{R}^{n-3}$.*

3 A noncontractible closure

As a brief final note, we give an example in which the space X_E of embedded polygons is contractible, but its closure $\overline{X}_E$ is not. This gives a negative resolution to a conjecture posed by Connelly, Demaine, and Rote [**6**, p. 235].

For the example, consider quadrilaterals with side lengths $\vec{\ell} = (6, 4, 2, 4)$. The main point is that all configurations of these quadrilaterals are embeddings with one exception, which occurs when the edges are folded over to lie along a line.

The full configuration space X is homeomorphic to a figure eight. One of the lobes consists of all the counterclockwise embeddings together with a straight line configuration which represents the point at which the two lobes are attached. This is illustrated in Figure 11. (The second lobe consists of the reflections of the first in the side of length 6.) Thus X_E is homeomorphic to a circle with a point deleted, which is contractible, while $\overline{X}_E$ is homeomorphic to a circle, which is not.

Of course, this example involves a straight line configuration, which we have

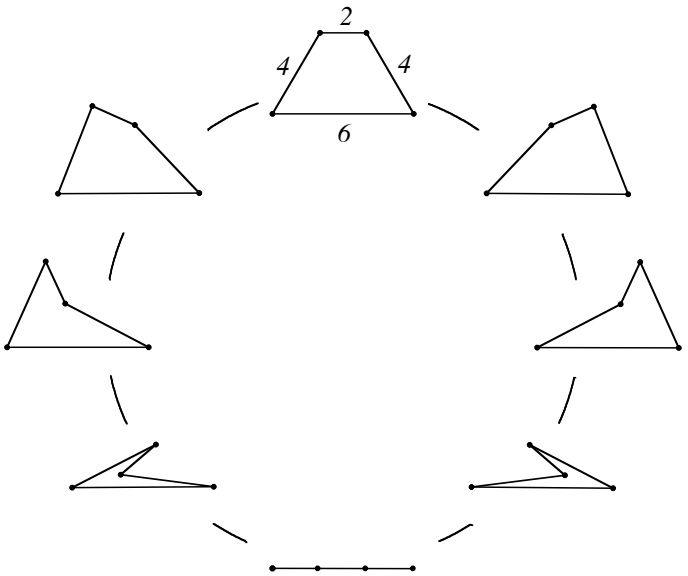

Figure 11: A circle of quadrilaterals with side lengths $6, 4, 2, 4$.

been excluding until now. Whether there is an example in which straight line configurations are not allowed remains to be seen.

References

[1] O. Aichholzer, E. Demaine, J. Erickson, F. Hurtado, M. Overmars, M. Soss, G. Toussaint, Reconfiguring convex polygons, *Computational Geometry: Theory and Applications* 20 (2001) 69–84.

[2] M. Brown, The monotone union of open n-cells is an open n-cell, *Proceedings of the American Mathematical Society* 12 (1961) 812–814.

[3] M. Brown, Locally flat imbeddings of topological manifolds, *Annals of Mathematics* 75 (1962) 331–341.

[4] J. H. Cantarella, E. D. Demaine, H. N. Iben, and J. F. O'Brien, An energy-driven approach to linkage unfolding, in *Proceedings of the 20th ACM Symposium on Computational Geometry*, J. Snoeyink and J-D. Boissonna, eds., ACM Press, New York, 2004, pp. 134–143.

[5] R. Connelly, A new proof of Brown's collaring theorem, *Proceedings of the American Mathemical Society* 27 (1971) 180–182.

[6] R. Connelly, E. Demaine, and G. Rote, Straightening polygonal arcs and convexifying polygonal cycles, *Discrete and Computational Geometry* 30 (2003) 205–239.

[7] J.-C. Hausmann, Sur la topologie des bras articules, in *Algebraic Topology, Poznán, 1989*, Lectures Notes in Mathematics, no. 1474, Springer-Verlag, Berlin, 1991, pp. 146–159.

[8] Y. Kamiyama, Topology of equilateral polygon linkages, *Topology and Its Applications* 68 (1996) 13-31.

[9] M. Kapovich and J. Millson, On the moduli space of polygons in the euclidean plane, *Journal of Differential Geometry* 42 (1995) 430–464.

[10] W. J, Lenhart and S. H. Whitesides, Reconfiguring closed polygonal chains in Euclidean d-space, *Discrete and Computational Geometry* 13 (1995) 123–140.

[11] J. Milnor, Differential topology, in *Lectures on Modern Mathematics*, vol. II, T. L. Saaty, ed., John Wiley and Sons, New York, 1964, pp. 165–183.

[12] D. Shimamoto and C. Vanderwaart, Spaces of polygons in the plane and Morse theory, *American Mathematical Monthly* 112 (2005) 289–310.